Supporting Information

Theoretical Study on Transition Metal Oxoboryl Complexes: M-BO Bonding Nature, Mechanism of the Formation Reaction, and Prediction of New Complexes

Guixiang Zeng and Shigeyoshi Sakaki*

Fukui Institute for Fundamental Chemistry, Kyoto University, Takano-Nishihiraki-cho 34-4, Sakyo-ku, Kyoto 606-8103, Japan

Complete representation of Ref. 39.

Frisch, M. J.; Trucks, G. W.; Schlegel, H. B.; Scuseria, G. E.; Robb, M. A.; Cheeseman, J. R.; Scalmani, G.; Barone, V.; Mennucci, B.; Petersson, G. A.; Nakatsuji, H.; Caricato, M.; Li, X.; Hratchian, H. P.; Izmaylov, A. F.; Bloino, J.; Zheng, G.; Sonnenberg, J. L.; Hada, M.; Ehara, M.; Toyota, K.; Fukuda, R.; Hasegawa, J.; Ishida, M.; Nakajima, T.; Honda, Y.; Kitao, O.; Nakai, H.; Vreven, T.; Montgomery, Jr., J. A.; Peralta, J. E.; Ogliaro, F.; Bearpark, M.; Heyd, J. J.; Brothers, E.; Kudin, K. N.; Staroverov, V. N.; Kobayashi, R.; Normand, J.; Raghavachari, K.; Rendell, A.; Burant, J. C.; Iyengar, S. S.; Tomasi, J.; Cossi, M.; Rega, N.; Millam, N. J.; Klene, M.; Knox, J. E.; Cross, J. B.; Bakken, V.; Adamo, C.; Jaramillo, J.; Gomperts, R.; Stratmann, R. E.; Yazyev, O.; Austin, A. J.; Cammi, R.; Pomelli, C.; Ochterski, J. W.; Martin, R. L.; Morokuma, K.; Zakrzewski, V. G.; Voth, G. A.; Salvador, P.; Dannenberg, J. J.; Dapprich, S.; Daniels, A. D.; Farkas, Ö.; Foresman, J. B.; Ortiz, J. V.; Cioslowski, J.; Fox, D. J. Gaussian, Inc., Wallingford CT, 2009.

Reliability of the B3LYP Functional

As shown in Figure S1, the B3LYP−optimized Pt−B and B−O bond distances in the oxoboryl complex $PtBr(BO)(PMe_3)_2$ are 1.970 and 1.217 Å, respectively, which agree well with the experimental values, 1.983 and 1.210 Å. The B−O stretching frequecy is calculated to be 1855 cm^{-1}, where the scale factor of 0.9806 was employed.[s1] This value agrees with the experimental BO streching frequency of 1853cm^{-1}. These results indicate that the DFT(B3LY)−optimized geometry is reliable.

To check the reliability of the energy barrier (E_a) and reaction energy (ΔE) calculated by DFT (B3LYP). The following formation reaction (Eq. S1) of the oxoboryl complex was investigated with DFT (LC−XLYP,[S2] M06L,[S3] M06,[S4] and M062x[S4]), MP2 to MP4(SDQ), SCS−MP2,[S5] and QCISD[S6] methods, where PH_3 was employed as a simple model of phosphine ligand.

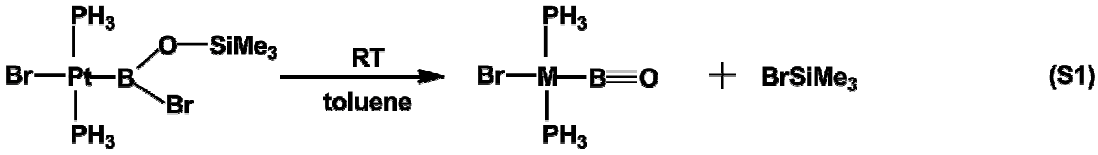

(S1)

The DFT(B3LYP)/BS−II calculated E_a and ΔE are 35.9 and 10.9 kcal/mol, respectively, as listed in Table S1. Optimized structural parameters are provided in the Table S2. It is noted that the E_a and ΔE values converge when going from MP2 to MP4(SDQ). The E_a value is 33.9 kcal/mol in both MP4(SDQ) and QCISD calculations. The QCISD−calculated ΔE value (14.7 kcal/mol) is not different very much from the MP4(SDQ)−calculated value (10.6 kcal/mol) and the other ΔE values are between them except for the LC−BLYP and M06 calculated values. These results indicate that the E_a value is almost 34 kcal/mol and the ΔE is between 10.6 and 14.7 kcal/mol. The B3LYP−calculated E_a and ΔE values are similar to these values, suggesting that energy changes calculated at the DFT(B3LYP)/BS−II level are reliable in the present system. Considering all these results, we will present discussion based on computational results obtained at the DFT(B3LYP)/BS−II level.

References

S1. Scott, A. P. ; Radom, L. *J. Phys. Chem.* **1996**, *100,* 16502.

S2. Iikura, H.; Tsuneda, T.; Yanai, T.; Hirao, K. *J. Chem. Phys.* **2001**, *115*, 3540.

S3. Zhao, Y.; Truhlar, D. G. *J. Chem. Phys.* **2006**, 125, 194101.

S4. Zhao, Y.; Truhlar, D. *Theor. Chem. Acc.* **2008**, *120*, 215.

S5. (a) King, R. A. *Mol. Phys.* **2009**, *107*, 789. (b) Grimme, S. *J. Chem. Phys.* **2003**, *118*, 9095. (c) Takatani, T.; Sherrill, C. D. *Phys. Chem. Chem. Phys.* **2007**, *9*, 6106.

S6. (a) Gauss, J.; Cremer, D. *Chem. Phys. Lett.* **1988**, *150* , 280. (b) Salter, E. A.; Trucks, G. W.; Bartlett, R. J. *J. Chem. Phys.* **1989**, *90*, 1752.

Table S1. Activation Barrier (E_a)[a] and Reaction Energy (ΔE)[b] of Formation Reaction of Oxoboryl Complex $PtBr(BO)(PH_3)_2$.

Methods	E_a [c]	ΔE [c]
B3LYP	35.9	10.9
LC−BLYP	39.2	17.4
M06	35.1	16.9
M06L	33.6	15.0
MP2	33.7	12.5
SCS−MP2	38.2	14.4
MP3	34.9	11.4
MP4(DQ)	35.1	11.0
MP4(SDQ)	33.9	10.6
QCISD	33.9	14.7

[a]The energy difference between the transition state and the precursor complex.

[b]The energy difference between the reactant and the sum of products.

[c] Without zero point energy correction, in kcal/mol unit. Solvent effect (toluene) was considered with the PCM method.

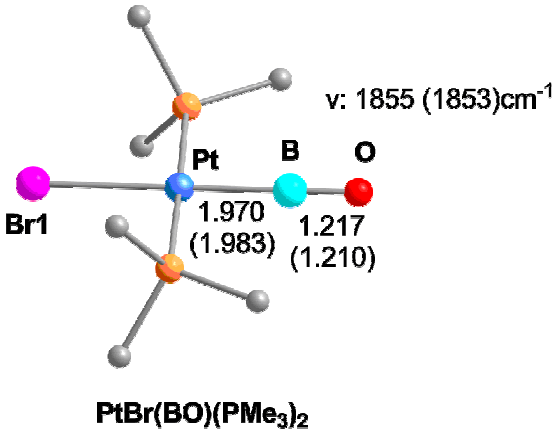

Figure S1. Optimized structure of $PtBr(BO)(PMe_3)_2$. Distances are in Å. Experimental data are in the parentheses.

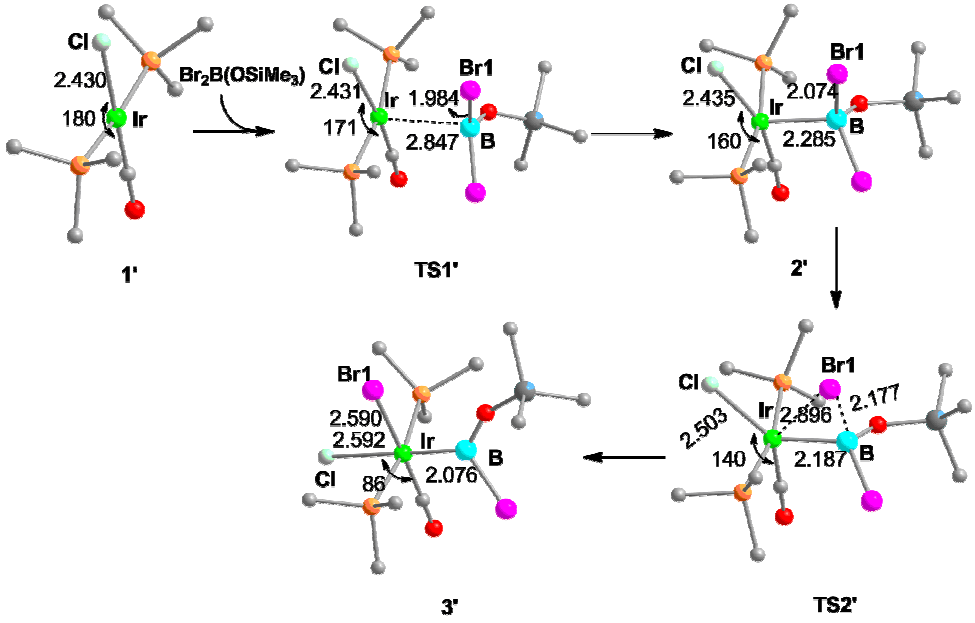

Figure S2. Optimized structure of the all species involved in the B–Br σ–bond oxidative addition to the Ir center in the Vaska–type complex $IrClBr(CO)(PMe_3)_2$. Distances are in Å. Angles marked by double arrows are in degree.

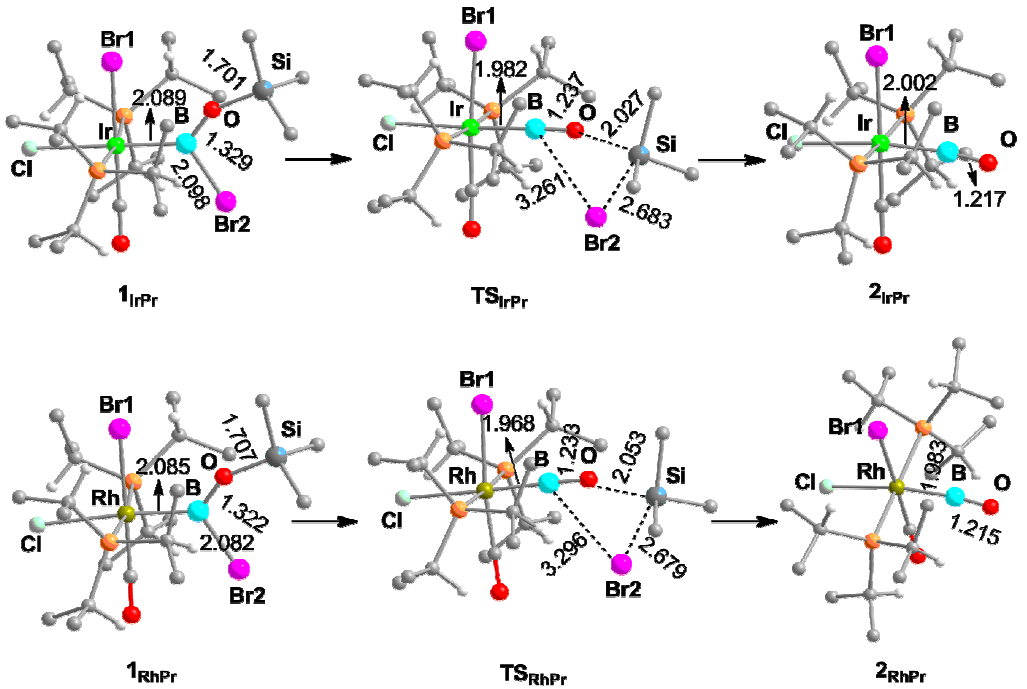

Figure S3. Optimized structures of all species involved in the formation reaction of oxoboryl complex MClBr(BO)(CO)[P(*i*–Pr)$_3$]$_2$ (M= Ir and Rh). H atoms on *i*–Pr and three methyl groups on Si are omitted for clarity. All the distances are in Å.

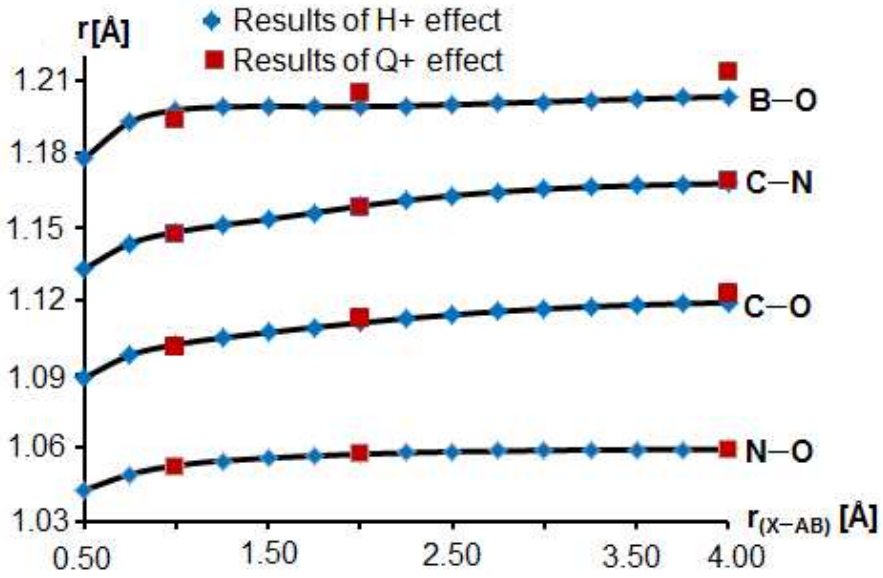

Figure S4. Calculated interatomic bond distance against various X–AB (AB represent the diatomic molecule) distance ($X=H^+$ or point charge Q^+).

Table S2. Optimized geometry parameters of reactants, transition states, and the oxoboryl products for L=CF_3, H, and *i*–Pr systems. Distances are in Å.

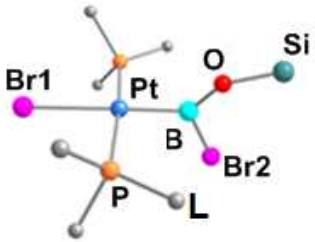

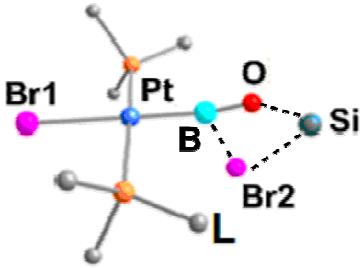

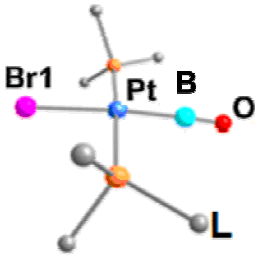

	CF_3	H	*i*–Pr	CF_3	H	*i*–Pr	CF_3	H	*i*–Pr
Br1–Pt	2.626	2.638	2.712	2.602	2.585	2.609	2.566	2.581	2.635
Pt–B	2.061	2.026	1.997	2.021	1.968	1.934	2.001	1.985	1.958
B–O	1.318	1.330	1.340	1.254	1.253	1.237	1.208	1.213	1.220
B–Br2	2.008	2.043	2.089	2.373	2.657	3.563			
O–Si	1.713	1.703	1.696	2.175	2.008	2.011			
Br2–Si	3.884	3.760	3.766	2.638	2.731	2.626			

Table S3. Electronic energies (E_s) of $[PtBr(PMe_3)_2]^+$, $[PtBr(PMe_3)_2]^-$, BO^-, and BO^+. All these species are fully optimized in the gas phase using B3LYP. Singlet point calculations were carried out in the solvent phase (toluene) with PCM model.

Species	E_s(a.u.)
$[PtBr(PMe_3)_2]^+$	-3615.787749
BO^-	-100.2011008
$[PtBr(PMe_3)_2]^-$	-3616.085107
BO^+	-99.644571

Table S4. B3LYP–calculated electronic energies in toluene solvent ($E_{sol,}$ in a.u.), zero–point energy (ZPE, in a.u.), entropies (in cal·(mol·k)$^{-1}$), and thermal correction energies(E_{therm} in kcal/mol, calculated at 298.15 K and 1 atm) for all stationary points involved in the formation reaction of M(Br)(BO)(PL_3)$_2$ (M=Pt, Pd, and Ni). **W–S_t** stands for the translational entropy calculated using Whitesides method, hereafter.

Species	E_{sol}	ZPE	W–S_t	S_r	S_v	E_{therm}
$\mathbf{1_{PtMe}}$	-6699.75341	0.35332	40.86	35.63	124.18	241.06
$\mathbf{TS_{PtMe}}$	-6699.70211	0.35300	40.86	35.69	121.21	240.53
$\mathbf{2_{PtBO}}$	-3716.21099	0.2393	39.99	33.21	76.56	163.21
3	-2983.53033	0.11246	36.74	28.34	22.38	76.10
$\mathbf{1_{PtCF3}}$	-8486.51001	0.21317	42.13	38.02	189.56	161.29
$\mathbf{TS_{PtCF3}}$	-8486.44315	0.21231	42.13	38.10	186.04	160.53
$\mathbf{2_{PtCF3}}$	-5502.95045	0.69759	41.60	36.93	143.37	83.47
$\mathbf{1_{PtPr}}$	-7171.55095	0.69759	41.59	37.37	185.04	466.93
$\mathbf{TS_{PtPr}}$	-7171.50779	0.69655	41.59	37.68	187.74	466.25
$\mathbf{2_{PtPr}}$	-4188.02037	0.58332	40.94	35.99	139.62	388.99
$\mathbf{1_{PdMe}}$	-6708.26133	0.35287	40.38	35.60	124.73	240.89
$\mathbf{TS_{PdMe}}$	-6708.20574	0.35230	44.61	35.62	122.45	240.27
$\mathbf{2_{PdMe}}$	-3724.71604	0.23878	39.34	33.21	77.86	163.03
$\mathbf{1_{NiMe}}$	-6751.25941	0.35332	40.09	35.37	121.28	240.96
$\mathbf{TS_{NiMe}}$	-6751.20568	0.35320	40.09	35.38	111.49	239.93
$\mathbf{2_{NiMe}}$	-3767.71694	0.23956	38.92	32.97	74.38	163.22

Table S5. B3LYP–calculated electronic energies in toluene solvent ($E_{sol,}$ in a.u.), zero–point energy (ZPE, in a.u.), entropies (in cal·(mol·k)$^{-1}$), and thermal correction energies(E_{therm} in kcal/mol, calculated at 298.15 K and 1 atm) for all stationary points involved in the formation reaction of M(Cl)(Br)(CO)(BO)$(PMe_3)_2$ (M=Ir and Rh). **W–S_t** stands for the translational entropy calculated using Whitesides method, hereafter.

Species	E_{sol}	ZPE	W–S_t	S_r	S_v	E_{therm}
1'	-1600.49041	0.24071	39.68	32.68	72.39	163.70
TS1'	-7258.38777	0.36331	41.14	36.04	134.71	249.30
2'	-7258.39243	0.36357	41.14	35.89	135.81	249.80
TS2'	-7258.38935	0.36356	41.14	35.87	130.61	249.27
1_{IrMe} (3')	-7258.41330	0.36482	41.14	35.92	133.33	250.37
TS_{IrMe}	-7258.3618	0.36429	41.14	36.14	133.59	249.82
2_{IrMe}	-4274.87141	0.25060	40.37	33.86	88.51	172.46
1_{RhMe}	-7264.57000	0.36414	41.46	35.85	135.72	250.13
TS_{RhMe}	-7264.51633	0.36334	41.46	36.08	135.32	249.47
2_{RhMe}	-4281.02714	0.24996	40.55	33.84	89.42	172.22

Table S6. M06L–calculated Gibbs Activation Energy ($\Delta G^{0‡}$)[a], Gibbs Reaction Energy (ΔG^0)[b], and Total Enthalpy Change (ΔH^0) for the Formation Reaction of the Oxoboryl Complex, $MBr(BO)(PR_3)_2$.

M	PR_3	$\Delta G^{0‡}$	ΔG^0
	$P(CF_3)_3$	40.9	12.1
Pt	PMe_3	29.9	1.0
	$P(i\text{–}Pr)_3$	26.8	-3.0
Pd	PMe_3	32.4	3.0
Ni	PMe_3	33.6	3.9
Ir	$P(i\text{–}Pr)_3$	27.9	0.8
Rh	$P(i\text{–}Pr)_3$	28.5	1.1

a.